NIH Public Access
Author Manuscript
Cancer Prev Res (Phila). Author manuscript; available in PMC 2013 September 01.

Published in final edited form as:
Cancer Prev Res (Phila). 2012 September ; 5(9): 1103–1114. doi:10.1158/1940-6207.CAPR-11-0397.

Taxifolin suppresses UV-induced skin carcinogenesis by targeting EGFR and PI3-K

Naomi Oi[1], **Hanyong Chen**[1], **Myoung Ok Kim**[1,2], **Ronald A. Lubet**[3], **Ann M. Bode**[1], and **Zigang Dong**[1]

[1]The Hormel Institute, University of Minnesota, 801 16th Avenue NE, Austin, MN 55912, USA.

[2]School of Animal Science and Biotechnology, Kyungpook National University, Sangju, Korea.

[3]National Cancer Institute, Bethesda, MD 20892, USA.

Abstract

Skin cancer is one of the most commonly diagnosed cancers in United States. Taxifolin reportedly exerts multiple biological effects but the molecular mechanisms and direct target(s) of taxifolin in skin cancer chemoprevention are still unknown. *In silico* computer screening and kinase profiling results suggest that the epidermal growth factor receptor (EGFR), phosphatidyl inositol 3-kinase (PI3-K) and Src are potential targets for taxifolin. Pull-down assay results showed that EGFR, PI3-K and Src directly interacted with taxifolin *in vitro*, whereas taxifolin bound to EGFR and PI3-K but not to Src in cells. ATP-competition and *in vitro* kinase assay data revealed that taxifolin interacted with EGFR and PI3-K at the ATP binding pocket and inhibit their kinase activities. Western blot analysis showed that taxifolin suppressed UVB-induced phosphorylation of EGFR and Akt, and subsequently suppressed their signaling pathways in JB6 P+ mouse skin epidermal cells. Expression levels and promoter activity of COX-2 and prostaglandin E_2 (PGE_2) generation induced by UVB were also attenuated by taxifolin. The effect of taxifolin on UVB-induced signaling pathways and PGE_2 generation was reduced in EGFR knockout murine embryonic fibroblasts (MEFs) compared with EGFR wildtype MEFs. Taxifolin also inhibited EGF-induced cell transformation. Importantly, topical treatment of taxifolin to the dorsal skin significantly suppressed tumor incidence, volume and multiplicity in a solar-UV (SUV)-induced skin carcinogenesis mouse model. Further analysis showed that the taxifolin-treated group had a substantial reduction in SUV-induced phosphorylation of EGFR and Akt in mouse skin. These results suggest that taxifolin exerts chemopreventive activity against UV-induced skin carcinogenesis by targeting EGFR and PI3-K.

Keywords

taxifolin; EGFR; PI3-K; skin carcinogenesis

Introduction

Skin cancer is one of the most common cancers in the United States. Each year over 1,000,000 new cases of skin cancers are reported in the United States making up 40% of all diagnosed cancers (1). Chronic ultraviolet (UV) exposure is recognized as a major etiologic factor of skin carcinogenesis (2). The UV spectrum can be divided into 3 wavelengths, UVA

Corresponding author: Zigang Dong, The Hormel Institute, University of Minnesota, 801 16th Ave NE, Austin, MN 55912. Phone: 507-437-9600; FAX: 507-437-9606; zgdong@hi.umn.edu.

Potential conflicts of interest: No potential conflicts of interest

(320–400 nm), UVB (280–320 nm) and UVC (200–280 nm) (3–4). Although UVC is filtered out by the ozone layer, UVA and UVB reach the earth's surface. Of the UV irradiation that reaches the surface of the earth, 90–99% is comprised of UVA and 1–10% is comprised of UVB (4). UVA is carcinogenic and causes photoaging and wrinkling of the skin (5). UVB is mainly responsible for a variety of skin diseases including melanoma and nonmelanoma skin cancers because it is capable of triggering the initiation, promotion and progression phases of skin cancer (6–7). Therefore, targeting UV-induced signaling might be an effective strategy for preventing skin carcinogenesis.

The epidermal growth factor receptor (EGFR) is activated by UV radiation (8). EGFR is a member of receptor tyrosine kinase, and reported to be activated and/or overexpressed in variety of human cancers including UV-induced skin cancer (9–10). UV irradiation rapidly activates EGFR through the induction of EGFR ligands and the inactivation of cytoplasmic protein tyrosine phosphatases that maintains low basal levels of phosphorylated EGFR (11–13). UV-activated EGFR in turn activates a number of signaling cascades, including extracellular regulated kinases (ERKs), p38 kinase and c-Jun NH_2-terminal kinases (JNKs), which are known regulators of cell division (14–16). In response to UV irradiation, EGFR also activates phosphatidyl inositol-3-kinase (PI3-K), leading to Akt activation and suppression of apoptosis (17). Therefore, the EGFR and PI3-K/Akt signaling pathways are logical molecular targets for chemoprevention of UV-induced skin cancer.

Taxifolin, also known as dihydroquercetin, is a flavonone commonly found in onions (18), milk thistle (19), French maritime bark (20) and Douglas fir bark (21) as an aglycone or glycoside form. Taxifolin has multiple biological effects, including antioxidant and anti-inflammatory effects and plays a role in preventing cardiovascular disease (22–24). Recently, several studies have focused on taxifolin as a potential cancer chemopreventive agent. One study showed that aglycone form of taxifolin exerts chemopreventive effects through an antioxidant response element (ARE)-dependent mechanism in colon cancer cells (25). The taxifolin aglycone form is also reported to induce apoptosis in prostate cancer cells (26). Although these reports provide evidence that taxifolin might exert chemopreventive effects against several cancers, the molecular mechanisms and direct targets of taxifolin are still unclear. Herein, we report that taxifolin suppresses UVB-induced activation of signal transduction by directly inhibiting EGFR and PI3-K in JB6 P+ mouse skin epidermal cells. Moreover, taxifolin strongly suppresses tumor incidence in a solar UV (SUV)-induced skin carcinogenesis mouse model. Thus, taxifolin acts as an inhibitor of EGFR and PI3-K and is expected to have beneficial effects in the prevention of UV-induced skin carcinogenesis.

Materials and Methods

Chemicals

"The aglycone form of taxifolin was purchased from Sigma-Aldrich (>85%; 2R,3R-(+)-taxifolin, St. Louis, MO) for *in vitro* and cell-based experiments; and for the animal study, taxifolin was purchased from ENZO Life Sciences (>90%; (+)-taxifolin, Plymouth Meeting, PA). Active EGFR, PI3-K (p110δ/p85α) and Src proteins were from Millipore (Billerica, MA). The antibody to detect phosphorylated p38 (Tyr180/Tyr182) was purchased from BD Biosciences (Sparks, MD). Antibodies against total Src, p38, ERK1/2, JNKs, Akt, p90RSK and EGFR, and phosphorylated ERK1/2 (Thr202/Tyr204), JNKs (Thr183/Tyr185), Akt (Tyr308 and Ser473), MSK (Ser376), p90RSK (Thr359/Ser363) and EGFR (Tyr1068) were from Cell Signaling Biotechnology (Danvers, MA). The antibodies against total MSK, PI3-K (p110) and β-actin were obtained from Santa Cruz Biotechnology (Santa Cruz, CA). The prostaglandin E_2 (PGE_2) EIA kit, COX Inhibitor Screening Assay kit and antibody against COX-2 were purchased from Cayman Chemical (Ann Arbor, MI).

Cell culture and transfection

The JB6 P+ mouse epidermal cell line was purchased from American Type Culture Collection (ATCC) and cultured in Eagle's Minimum Essential Medium (MEM)/5% FBS. For the luciferase assay, the JB6 P+ cells were stably transfected with a *COX-2 luciferase reporter* plasmid and maintained in MEM/5% FBS containing 200 μg/ml G418 as described earlier (27). EGFR wildtype (EGFR/WT) and EGFR knockout (EGFR/KO) murine embryonic fibroblasts (MEFs) were cultured in Dulbecco's modified Eagle's medium (DMEM)/10% FBS as reported previously (28). All cells were cultured with antibiotics at 37°C in a CO_2 incubator. Cells were cytogenetically tested and authenticated before the cells were frozen. Each vial of frozen cells was thawed and maintained for a maximum of 8 weeks.

In silico target identification

To find the potential biological targets of taxifolin, a shape similarity method, a part of the PHASE module of Schrödinger's (29) molecular modeling software package, was used based on the chemical structure of taxifolin. The parameter of atom-type for volume was set to pharmacophore, which means that the queries were used not only to consider shape similarity but also to align potential pharmacophore points with the targets. The protein target library was obtained from the Protein Data Bank (30). To provide more structure orientations for possible alignment, we set the maximum number of conformers per molecule in the library to be generated at 100 while retaining up to 10 conformers per rotatable bond. We filtered out conformers with similarity below 0.7. Then we obtained the PDB ID associated with each aligned target molecule. The PDB ID could show us the protein type through the online Protein Data Bank.

Pull-down assays

Taxifolin-conjugated Sepharose 4B beads or Sepharose 4B beads were prepared as reported earlier (27). For *in vitro* or *ex vivo* pull-down assay, active EGFR, PI3-K or Src (200 ng) or lysates from JB6 P+ cells (500 μg) were mixed with 50 μl of taxifolin-conjugated Sepharose 4B beads or Sepharose 4B beads in reaction buffer [50 mM Tris–HCl (pH 7.5), 5 mM EDTA, 150 mM NaCl, 1 mM DTT, 0.01% NP-40, 2 μg/ml BSA, 0.02 mM PMSF and 1× protease inhibitor cocktail]. After incubation with gentle rocking at 4°C overnight, the beads were washed 5 times with washing buffer [50 mM Tris–HCl (pH 7.5), 5 mM EDTA, 150 mM NaCl, 1 mM DTT, 0.01% NP-40 and 0.02 mM PMSF], and then the proteins bound to the beads were analyzed by Western blot. For the ATP competition assay, active EGFR or PI3-K (200 ng) was incubated with different concentrations of ATP (0, 10 or 100 μM) in reaction buffer at 4°C overnight. Taxifolin-conjugated Sepharose 4B beads or Sepharose 4B beads were added and again incubated at 4°C overnight. After washing 5 times with washing buffer, the proteins bound to the beads were analyzed by Western blot.

In vitro EGFR kinase assay

The *in vitro* EGFR kinase assay was carried out in accordance with the instructions provided by Millipore. Active EGFR (100 ng) was mixed with taxifolin (0, 20, 40 or 80 μM) or erlotinib (10 μM, LC laboratories, Woburn, MA) in reaction buffer [40 mM MOPS/NaOH (pH 7.0), 1 mM EDTA, 10 mM $MnCl_2$ and 0.8 M ammonium sulphate]. Erlotinib, a well-known EGFR inhibitor, were used as a positive control. The mixture was incubated with 500 μM angiotensin II for 5 min at room temperature, followed by incubation with 10 μl of a ATP mixture [25 mM MgAc and 0.25 mM ATP containing 10 μCi [γ-^{32}P]ATP] for 20 min at 30°C and then 25 μl of reaction mixture were transferred onto P81 papers. The papers were washed with 1% phosphoric acid twice and with acetone once. The radioactive incorporation was determined using a scintillation counter.

In vitro PI3-K kinase assay

The *in vitro* PI3-K kinase assay was carried out as described earlier (31). Active PI3-K (100 ng) was incubated with taxifolin (0, 20, 40 or 80 μM) or LY294002 (10 μM) for 10 min at 30°C. LY 294002, a well-known PI3-K inhibitor, was used as a positive control. The mixtures were incubated with 0.5 mg/ml phosphatidylinositol (MP Biomedicals, Solon, OH) for 5 min at room temperature, followed by incubation with reaction buffer [10 mM Tris-HCl (pH 7.6), 60 mM $MgCl_2$ and 0.25 mM ATP containing 10 μCi [γ-^{32}P] ATP] for an additional 10 min at 30°C. The reaction was stopped by adding 15 μl of 4 N HCl and 130 μl of chloroform : methanol = 1 : 1. After mixing, the lower chloroform phase were spotted onto a silica gel plate (Merck KGaA, Darmstadt, Germany). The resulting ^{32}P-labeled phosphatidylinositol-3-phosphate (PI3P) was separated by thin layer chromatography with developing solvent [chloroform : methanol : NH_4OH : H_2O = 60 : 47 : 2 : 11.3] and then visualized by autoradiography.

Molecular modeling

The active wildtype EGFR tyrosine kinase domain (PDB ID:1m17) was chosen for docking studies. Its X-ray diffraction structure had a resolution of 2.6 Å (32) and erlotinib was bound to the ATP binding site of the EGFR. For PI3-K, the crystal structure of the murine P110δ in complex with ZSTK474 (PDB ID:2WXL) was chosen for docking studies. Its X-ray diffraction structure had a resolution of 1.99 Å. ZSTK474 is an ATP-competitive inhibitor and has a shape similarity with taxifolin of 0.67 (33). EGFR and PI3-K were prepared for docking using the Protein Preparation Wizard in the Schrödinger Suite 2010 using a standard procedure outlined separately. Taxifolin was prepared using MacroModel of Schrödinger and minimized and the lowest energy conformations for docking were determined by using default parameters. The protein-ligand docking analysis was performed using the Induced Fit docking program of Schrödinger, which can provide the ligand binding flexibility with the binding pocket residues. Images are generated with the UCSF Chimera program (34).

Cell viability assay

JB6 P+ cells (1×10^4) were cultured in 96-well plates and then treated with various concentrations of taxifolin (0, 20, 40 or 80 μM). After incubation for 24, 48 or 72 h, 20 μl of CellTiter96 Aqueous Non-Radioactive Cell Proliferation Assay Kit (Promega, Madison, WI) were added to each well. After additional incubation for 1 h at 37°C in a 5% CO_2 incubator, absorbance was measured at 490 and 690 nm.

UVB-irradiation

A UVB irradiation system (FS20 T12/UVB, National Biological corporation, Twinsburg, OH) was used to stimulate cells in serum-free medium. The spectral peak from the UVB source was at 311 nm.

Western blot

JB6 P+ cells (1×10^6) or MEFs (5×10^5) were cultured in 10-cm dishes and then starved in serum-free medium for 48 h. The cells were treated with various concentrations of taxifolin (0, 20, 40 or 80 μM), gefitinib (2 μM) and/or LY294002 (2 μM) for 24 h before exposure to UVB (4 kJ/m^2). The lysate proteins were subjected to SDS-PAGE and transferred to a polyvinylidene difluoride (PVDF) membrane. After blocking with 5% milk, the membrane was incubated with a specific primary antibody, and then protein bands were visualized by the ECL system after hybridization with a horseradish peroxidase-conjugated secondary antibody.

COX-2 luciferase assay

JB6 P+ cells stably transfected with a *COX-2 luciferase reporter* plasmid (8×10^3) were cultured in 96-well plates and then starved in serum-free medium for 24 h. The cells were treated with various concentrations of taxifolin (0, 20, 40 or 80 μM) for 1 h before exposure to UVB (4 kJ/m^2). After incubation for 12 h, the cells were disrupted with 100 μl of lysis buffer [0.1 M potassium phosphate buffer (pH 7.8), 1% Triton X-100, 1 mM DTT and 2 mM EDTA] and luciferase activity was measured using a luminometer (Luminoskan Ascent; Thermo Election).

PGE_2 assay

JB6 P+ cells or MEFs (1×10^5) were cultured in 6-well plates and then starved in serum-free medium for 24 h. The cells were treated with various concentrations of taxifolin (0, 20, 40 or 80 μM) or celecoxib (10 μM) for 1 h before exposure to UVB (4 kJ/m^2). After incubation for 6 h, the amount of PGE_2 released into the medium was measured using the PGE_2 EIA kit following the supplier's instructions. A standard curve with PGE_2 provided with the kit was generated at the same time. Celecoxib, a well-known inhibitor for COX-2, was used as a positive control.

In vitro COX-2 activity

In vitro COX-2 activity was determined by measuring the synthesis of PGs using the COX Inhibitor Screening Assay kit following the supplier's instructions. A standard curve with PGs was generated at the same time. Celecoxib was used as a positive control.

Cell transformation assay

JB6 P+ cells (8×10^3) were suspended in 1 ml of BME supplemented with 10% FBS and 0.33% agar and treated with various concentrations of taxifolin (0, 20, 40 or 80 μM), gefitinib (0.1 μM), LY294002 (1 μM) or celecoxib (10 μM) together with 1 ng/ml EGF on 3 ml of solidified BME supplemented with 10% FBS and 0.5% agar with the indicated concentrations of compound together with 1 ng/ml EGF. After incubation for 7 days in a CO_2 incubator, colonies were counted.

Animals

Female SKH-1 hairless mice (5–13 weeks old) were purchased from Charles River (Wilmington, MA). Animals were acclimated for 2 weeks before the study and had free access to food and water. All animal studies were performed according to guidelines approved by the University of Minnesota Institutional Animal Care and Use Committee (IACUC). The animals were housed in climate-controlled quarters with a 12 h light/12 h dark cycle.

Skin carcinogenesis was induced by an SUV irradiation system (SUV-340, Q-LAB, Cleveland, OH). SKH-1 mice were divided into 5 age-matched groups: Vehicle group (n = 10), 1.0 mg taxifolin group (n = 10), Veh/SUV group (n = 20), 0.5 mg taxifolin/SUV group (n = 20) and 1.0 mg taxifolin/SUV group (n = 20). In the Vehicle group, 200 μl of acetone was topically treated to the dorsal skin of mice and mice were not exposed to SUV. In the 1.0 mg taxifolin group, 1.0 mg taxifolin in 200 μl of acetone was topically treated to the dorsal skin and mice were not exposed to SUV. In the Veh/SUV group, the dorsal skin was topically treated with 200 μl of acetone before SUV irradiation. The mice in the 0.5 mg taxifolin/SUV or 1.0 mg taxifolin/SUV groups received topical application of taxifolin (0.5 or 1.0 mg) in 200 μl of acetone before SUV irradiation. The SUV irradiation was given 3 times a week for 15 weeks as described below. At week 1, mice were irradiated with SUV at a dose of 30 kJ/m^2 UVA and 1.8 kJ/m^2 UVB 3 times a week. The dose of SUV was

progressively increased (10% each week) due to the ensuing hyperplasia that can occur with SUV irradiation of the skin. At week 6, the dose of SUV reached 48 kJ/m^2 UVA and 2.9 kJ/m^2 UVB and this dose was maintained for week 6–15. Mice were weighed and tumors were measured by caliper once a week until week 30 or tumors reached 1 cm^3 total volume, at which time mice were euthanized and then skins were collected for further analysis.

Statistical analysis

All quantitative data are expressed as means ± S.D. or S.E. as indicated. The Student's *t*-test or a one-way ANOVA was used for statistical analysis. A probability of $P < 0.05$ was used as the criterion for statistical significance.

Results

EGFR and PI3-K are potential targets of taxifolin

To find potential molecular targets of taxifolin (Fig. 1A), we first performed *in silico* screening using a shape similarity method. Shape similarity scores of 15 proteins were over 0.7, suggesting that those proteins are potential targets of taxifolin (Supplemental Table. 1). We then performed *in vitro* kinase profiling (KinaseProfiler™ Millipore) with taxifolin against those proteins. Results indicated that the kinase activities of EGFR, PI3-K and Src were inhibited by over 50% by taxifolin at 80 μM (EGFR: 95%, PI3-K: 51% and Src: 53%, respectively). To determine whether taxifolin binds to EGFR, PI3-K or Src, *in vitro* and *ex vivo* pull-down assays were performed. Recombinant EGFR, PI3-K and Src indeed interacted with taxifolin-Sepharose 4B beads *in vitro* (Fig. 1B). However, taxifolin-Sepharose 4B beads pulled down only EGFR and PI3-K, but not Src using cell lysates from JB6 P+ cells *ex vivo* (Fig. 1C). *In vitro* kinase assay results revealed that taxifolin suppressed kinase activities of EGFR (Fig. 1D) and PI3-K (Fig. 1E), and the IC_{50} value of taxifolin against EGFR or PI3-K was 29.0 μM or 78.4 μM, respectively. These results indicate that EFGR and PI3-K are effective targets of taxifolin.

Taxifolin binds to EGFR and PI3-K at the ATP-binding pocket

Our computer screening indicated that the shape and pharmacophore of taxifolin were similar with N-[4-(3–bromo-phenylamino)-quinazolin-6-yl]-acrylamide (PDB ID:2j5f), a known EGFR inhibitor, and with 4-amino-2-methyl-N-(1H-pyrazol-3-yl) quinazoline-8-carboxamide (PDB ID:3prz), a known PI3-K inhibitor (Supplemental Table 1). Both inhibitors were reported to interact with the ATP-binding pocket of the respective proteins. Therefore, taxifolin might also bind to the ATP-binding pocket. ATP-competition assays showed that the binding ability of taxifolin with EGFR (Fig. 2A) or PI3-K (Fig. 2B) was altered in the presence of ATP. We then docked taxifolin to EGFR or PI3-K using the Induced Fit Docking module of the Schrödinger Suite 2010 in extra precision. Taxifolin formed interactions within the ATP-binding pocket of EGFR (Fig. 2C) or PI3-K (Fig. 2D). The important hydrogen bonds with taxifolin were formed with Lys721, Met769 and Asp831 of EGFR and Lys779, Val828 and Asp911 of PI3-K, respectively. These results suggest that taxifolin is an ATP-competitive inhibitor of EGFR and PI3-K.

Taxifolin suppresses UVB-induced EGFR and PI3-K/Akt signaling pathways in JB6 P+ cells

To demonstrate the effect of taxifolin on UV-induced skin carcinogenesis, we first determined the cytotoxicity of taxifolin in the JB6 P+ mouse epidermal cell line. Taxifolin up to 80 μM had no cytotoxicity in JB6 P+ cells (Fig. 3A). Gefitinib, a well-known selective EGFR inhibitor, is reported to interact with EGFR at the ATP-binding pocket and suppresses EGFR kinase activity by attenuation of its autophosphorylation (35). According to our results showing that taxifolin binds to EGFR at the ATP-binding site (Fig. 2A, C),

taxifolin might also suppress autophosohorylation of EGFR. In fact, UVB-induced phosphorylation of EGFR at Tyr1068, which is an important auto-phosphorylation site of EGFR, is suppressed by taxifolin (Fig. 3B). Phosphorylation of Akt and p70S6K, PI3-K/Akt signaling proteins, was also suppressed by taxifolin (Fig. 3C). We then determined whether taxifolin could inhibit UVB-induced phosphorylation of ERKs, p38 and JNKs, well-known signaling kinases phosphorylated by EGFR in response to UV irradiation (14–16). Taxifolin suppressed UVB-induced phosphorylation of ERKs, p38 and JNKs (Fig. 3D) and also reduced phosphorylation of their down-stream target proteins, p90RSK, MSK and c-Jun (Fig. 3E). To confirm that the effects of taxifolin on these signaling proteins are related to the inhibition of EGFR and PI3-K, we used gefitinib or LY294002 as positive controls (Fig. 3C–E). Gefitinib suppressed phosphorylation of all the kinases induced by UVB including those in the PI3-K/Akt signaling pathway because EGFR also activates PI3-K/Akt signaling in response to UV irradiation (11, 24). LY294002 only suppressed phosphorylation of the PI3-K/Akt signaling pathway. These data suggest that taxifolin suppresses UVB-induced activation of the EGFR and PI3-K/Akt signaling pathways through inhibition of EGFR and PI3-K.

Taxifolin suppresses UVB-induced COX-2 through EGFR and PI3-K/Akt signaling in JB6 P + cells

The EGFR, as well as the PI3-K /Akt signaling pathways, are reported to enhance expression levels of cyclooxygenase-2 (COX-2) in response to UV irradiation (36–37). We therefore examined whether taxifolin could suppress UV-induced COX-2 expression and found that taxifolin suppressed UVB-induced COX-2 expression in a dose-dependent manner (Fig. 4A). Gefitinib and LY294002 suppressed COX-2 expression and co-treatment with gefitinib and LY294002 showed a stronger effect than treatment individually (Fig. 4A). Taxifolin also suppressed UVB-induced promoter activity of *COX-2* (Fig. 4B) and generation of PGE_2 (Fig. 4C), the enzyme product of COX-2, in JB6 P+ cells. To verify that taxifolin does not inhibit COX-2 directly, *in vitro* COX-2 activity was determined and results indicated that taxifolin had no effect on COX-2 activity *in vitro* (Fig. 4D). These results suggest that taxifolin regulates COX-2 through inhibition of EGFR and PI3-K.

The effect of taxifolin is reduced in EGFR/KO MEFs compared with EGFR/WT MEFs

Our *in vitro* kinase assay data showed that the IC_{50} values of taxifolin are 29.0 μM for EGFR and 78.4 μM for PI3-K, respectively (Fig. 1D, E), suggesting that EGFR is the major target of taxifolin. We therefore compared the effects of taxifolin in EGFR/WT and KO MEFs. Western blotting data verified that EGFR was only detected in EGFR/WT MEFs (Fig. 5A). Taxifolin suppressed UVB-induced phosphorylation of ERKs, p38, JNKs and Akt in EGFR/WT MEFs, whereas the effects of taxifolin on phosphorylation of ERKs, p38 and JNKs were not apparent in EGFR/KO MEFs (Fig. 5B). Phosphorylation of Akt was completely blocked in EGFR/KO MEFs and UVB-induced PGE_2 generation was strongly down-regulated by knocking down EGFR expression (Fig.5C). The effect of taxifolin on UVB-induced PGE_2 generation was also not obvious in EGFR/KO MEFs compared with EGFR/WT MEFs (Fig.5C). These results suggest that EGFR is a major target of taxifolin in UVB-induced skin carcinogenesis. The UV spectrum can be divided into UVA (320>–400 nm), UVB (280–320 nm) and UVC (200–280 nm) (3–4). Because the UV **ectrum (max) of taxifolin is = 289 ± 2 nm, at least a portion of the effect of taxifolin could be due to UV absorption. To address this issue, we determined whether taxifolin could inhibit epidermal growth factor (EGF)-induced cell transformation and results indicated that taxifolin suppressed EGF-induced cell transformation (Fig. 5D). Gefitinib and LY294002, as well as celecoxib, also suppressed EGF-induced cell transformation and co-treatment with gefitinib and LY294002 showed a stronger effect than individual drug treatment. These results

indicate that taxifolin also suppresses cell transformation induced by EGFR stimulation and not only affects the UV-induced signaling pathways.

Taxifolin suppresses SUV-induced skin carcinogenesis in SKH-1 hairless mice *in vivo*

To investigate the chemopreventive effect of taxifolin *in vivo*, we used the SUV-induced skin carcinogenesis mouse model. Although UVB is a major etiological factor for the development of skin cancer, UVA is the most abundant component of UV irradiation (4). SUV irradiation consists of UVA and UVB, and more closely resembles the natural environment than UVB only. At first, we confirmed that taxifolin indeed suppressed SUV-induced COX-2 expression (Supplemental Fig. 2A) and PGE_2 generation (Supplemental Fig. 2B). We then investigated the chemopreventive effect of taxifolin in the SUV-induced skin carcinogenesis mouse model. Topical application of taxifolin on mouse skin resulted in a substantial inhibition of SUV-induced tumor incidence (Fig. 6A). Topical application of taxifolin decreased the average tumor volume per mouse (Fig. 6B) and also significantly reduced tumor multiplicity at week 30 (Fig. 6C). Western blot analysis of the mouse skin showed that phosphorylation of EGFR and Akt and COX-2 expression induced by SUV were dramatically suppressed in the taxifolin-treated group (Fig. 6D). Taxifolin also strongly suppressed SUV-induced PGE_2 generation in mouse skin (Fig. 6E). These results clearly showed that taxifolin exerts a strong preventive effect against SUV-induced mouse skin carcinogenesis through inhibition of EGFR and PI3-K activation.

Discussion

Taxifolin has been reported to exert chemopreventive effects on several cancers. However, the mechanism and direct targets of taxifolin have not been elucidated. In the present study, we report that taxifolin directly inhibits the kinase activities of EGFR and PI3-K, and exerts strong chemopreventive effects against UV-induced skin carcinogenesis. Several studies have shown that the EGFR and PI3-K/Akt signaling pathways are critical for UV-induced skin carcinogenesis. EGFR is activated and/or overexpressed in a variety of human cancers including UV-induced skin cancer (9–10), and AG1478, a specific inhibitor of EGFR, was shown to prevent UV-induced skin carcinogenesis (14). UV-irradiation also was reported to suppress mitochondria- and caspase-dependent apoptosis through the PI3-K/Akt pathway and PI3-K inhibitors, LY294002 and wartmannin, suppressed the rescue from apoptosis by UV irradiation (38). Therefore, our finding suggests the usefulness of taxifolin in UV-induced skin cancer prevention by direct inhibition of EGFR and PI3-K.

According to our in *sillico* computer screening and kinase profiling data, we identified EGFR, PI3-K and Src as potential targets of taxifolin (Supplemental Table. 1). *In vitro* pull-down data showed that taxifolin pulled down EGFR, PI3-K and Src, whereas taxifolin only pulled down EGFR and PI3-K when taxifolin was incubated with cell lysates *ex vivo* (Fig. 1B, C). These results suggest that the binding affinity of taxifolin with Src is lower than with EGFR and PI3-K. Therefore, we conclude that EGFR and PI3-K are targets of taxifolin. The IC_{50} value of taxifolin against those kinase activities *in vitro* was 29.0 μM for EGFR and 78.4 μM for PI3-K, respectively (Fig. 1D, E). The effect of taxifolin on UV-induced phosphorylation of ERKs, JNKs and p38 completely disappeared in EGFR/KO MEFs (Fig. 5B), and inhibition of UV-induced PGE_2 generation by taxifolin were also not apparent in EGFR/KO MEFs (Fig. 5C). These results suggest that EGFR is a major effective target of taxifolin.

Taxifolin is found in an aglycone or glycoside form at different levels in various plants, including onions (18), milk thistle (19), French maritime bark (20) and Douglas fir bark (21). For example, the aglycon form was extracted at 97.1 mg/kg and the taxifolin-7-gluoside form at 5.8 mg/kg from the bulbs of red onion (18) and very high levels of the

aglycon form (620 mg/kg) are found in the seed of milk thistle (19). Because taxifolin has two chiral carbon centers, four enantiomeric forms of taxifolin are possible, 2S3R-(+), 2S3S-(−), 2R3R-(+) and 2R3S-(−)-taxifolin (39). Many studies that have considered enantio-separation of taxifolin did not separate the four enantiomers, but only two enantiomers (39–41). Vega-Villa et al. (39) successfully separated four enantiomers of taxifolin and their glycosides using reversed-phase high performance liquid chromatography (RP-HPLC). They indicated that 2R3R-(+)-taxifolin is a major taxifolin enantiomer in tu fu ling (*Rhizoma smilacis glabrae*, which has been used in traditional Chinese medicine to treat cancer and AIDS patients (42). Engelhardtia chrysolepis, which is also a traditional Chinese medicine, mainly contains 2R3R-(+)-taxifolin as astilbin (2R3R-(+)-taxifolin rhamnoside) (22). In the present study, we used 2R3R-(+)-taxifolin for *in vitro* and cell-based experiments, and (+)-taxifolin (2R3R, 2S3R-(+)-taxifolin) for the *in vivo* study. The purities of 2R3R-(+)-taxifolin and (+)-taxifolin are 85% and 90%, respectively. These low purities are because of the difficulty of separation of four taxifolin enantiomers. We therefore compared the docking score of each of the 4 taxifolin enantiomers against EGFR or PI3-K by computer modeling. All 4 taxifolin enantiomers interact with EGFR and PI3-K with a similar docking score (Supplemental Table 2). We therefore conclude that even though taxifolin enantiomers are probably contaminants, these enantiomers likely also have the ability to inhibit the kinase activity of EGFR or PI3-K.

Our results showed that taxifolin suppressed UVB-induced phosphorylation of EGFR signaling as well as the PI3-K/Akt signaling pathways (Fig 3B-E). Previous studies indicate that UV-induced the EGFR and PI3-K/Akt signaling pathways play important regulatory roles in COX-2 expression and PGE_2 generation (36–37). COX-2, a rate-limiting enzyme for oxidative conversion of arachidonic acid to prostaglandins, is recognized as a critical enzyme for enhancing cell proliferation, angiogenesis and tumor promotion (2, 43). In human and murine skin cells, COX-2 is up-regulated in response to acute and chronic UVB irradiation (37), and a selective COX-2 inhibitor strongly suppresses UV-induced skin carcinogenesis (44). Importantly, direct inhibitors of EGFR or PI3-K reduce UVB-induced skin carcinogenesis by down-regulation of COX-2 expression (36). We therefore investigated whether the inhibition of EGFR and PI3-K/Akt pathways by taxifolin affects COX-2 expression. Our results indicated that UVB-induced COX-2 expression and PGE_2 generation were suppressed by taxifolin (Fig. 4A,B). Consistent with previous reports, selective inhibitors of EGFR or PI3-K showed strong inhibition of UVB-induced COX-2 expression. These results suggest that taxifolin suppresses UV-induced COX-2 expression by inhibition of EGFR and PI3-K. Wang et al. (24) reported that taxifolin suppressed lipopolysaccharide (LPS)-induced COX-2 expression. However, no information regarding the direct target of taxifolin was included. LPS is reported to mediate enhanced COX-2 expression through the activation of EGFR (45). Sheu *et al.* also demonstrated that the PI3-K/Akt signaling pathway is involved in COX-2 expression and cell proliferation induced by LPS (46). These reports support our finding that taxifolin suppresses COX-2 expression through inhibition of EGFR and PI3-K. Overall, our study showed that taxifolin exerted excellent inhibitory effects against UV-induced skin by directly targeting EGFR and PI3-K. Thus, taxifolin is expected to have highly beneficial effects in the prevention of skin carcinogenesis.

Supplementary Material

Refer to Web version on PubMed Central for supplementary material.

Acknowledgments

Financial support: This work was supported by the Hormel Foundation and National Institutes of Health grants: R37 CA081064, CA027502, CA120388, ES016548.

References

1. Ricotti C, Bouzari N, Agadi A, Cockerell CJ. Malignant skin neoplasms. Med Clin North Am. 2009; 93:1241–1264. [PubMed: 19932329]
2. Buckman SY, Gresham A, Hale P, Hruza G, Anast J, Masferrer J, et al. COX-2 expression is induced by UVB exposure in human skin: implications for the development of skin cancer. Carcinogenesis. 1998; 19:723–729. [PubMed: 9635856]
3. de Gruijl FR. Photocarcinogenesis: UVA vs UVB. Methods Enzymol. 2000; 319:359–366. [PubMed: 10907526]
4. Matsui MS, DeLeo VA. Longwave ultraviolet radiation and promotion of skin cancer. Cancer Cells. 1991; 3:8–12. [PubMed: 2025494]
5. Nichols JA, Katiyar SK. Skin photoprotection by natural polyphenols: anti-inflammatory, antioxidant and DNA repair mechanisms. Arch Dermatol Res. 2010; 302:71–83. [PubMed: 19898857]
6. Bode AM, Dong Z. Mitogen-activated protein kinase activation in UV-induced signal transduction. Sci STKE. 2003; 2003:RE2. [PubMed: 12554854]
7. Matsumura Y, Ananthaswamy HN. Toxic effects of ultraviolet radiation on the skin. Toxicol Appl Pharmacol. 2004; 195:298–308. [PubMed: 15020192]
8. Rosette C, Karin M. Ultraviolet light and osmotic stress: activation of the JNK cascade through multiple growth factor and cytokine receptors. Science. 1996; 274:1194–1197. [PubMed: 8895468]
9. Gullick WJ. Prevalence of aberrant expression of the epidermal growth factor receptor in human cancers. Br Med Bull. 1991; 47:87–98. [PubMed: 1863851]
10. Scaltriti M, Baselga J. The epidermal growth factor receptor pathway: a model for targeted therapy. Clin Cancer Res. 2006; 12:5268–5272. [PubMed: 17000658]
11. Coffer PJ, Burgering BM, Peppelenbosch MP, Bos JL, Kruijer W. UV activation of receptor tyrosine kinase activity. Oncogene. 1995; 11:561–569. [PubMed: 7543196]
12. Huang RP, Wu JX, Fan Y, Adamson ED. UV activates growth factor receptors via reactive oxygen intermediates. J Cell Biol. 1996; 133:211–220. [PubMed: 8601609]
13. Xu Y, Shao Y, Voorhees JJ, Fisher GJ. Oxidative inhibition of receptor-type protein-tyrosine phosphatase kappa by ultraviolet irradiation activates epidermal growth factor receptor in human keratinocytes. J Biol Chem. 2006; 281:27389–27397. [PubMed: 16849327]
14. El-Abaseri TB, Fuhrman J, Trempus C, Shendrik I, Tennant RW, Hansen LA. Chemoprevention of UV light-induced skin tumorigenesis by inhibition of the epidermal growth factor receptor. Cancer Res. 2005; 65:3958–3965. [PubMed: 15867397]
15. El-Abaseri TB, Putta S, Hansen LA. Ultraviolet irradiation induces keratinocyte proliferation and epidermal hyperplasia through the activation of the epidermal growth factor receptor. Carcinogenesis. 2006; 27:225–231. [PubMed: 16123117]
16. Peus D, Vasa RA, Meves A, Beyerle A, Pittelkow MR. UVB-induced epidermal growth factor receptor phosphorylation is critical for downstream signaling and keratinocyte survival. Photochem Photobiol. 2000; 72:135–140. [PubMed: 10911738]
17. Wan YS, Wang ZQ, Shao Y, Voorhees JJ, Fisher GJ. Ultraviolet irradiation activates PI 3-kinase/AKT survival pathway via EGF receptors in human skin in vivo. Int J Oncol. 2001; 18:461–466. [PubMed: 11179472]
18. Slimestad R, Fossen T, Vagen IM. Onions: a source of unique dietary flavonoids. J Agric Food Chem. 2007; 55:10067–10080. [PubMed: 17997520]
19. Wallace SN, Carrier DJ, Clausen EC. Batch solvent extraction of flavanolignans from milk thistle (Silybum marianum, L. Gaertner). Phytochem Anal. 2005; 16:7–16. [PubMed: 15688950]

20. Rohdewald P. A review of the French maritime pine bark extract (Pycnogenol), a herbal medication with a diverse clinical pharmacology. Int J Clin Pharmacol Ther. 2002; 40:158–168. [PubMed: 11996210]
21. Kiehlmann E, Li EPM. Isomerization of Dihydroquercetin. J Nat Products. 1995; 58:450–455.
22. Haraguchi H, Mochida Y, Sakai S, Masuda H, Tamura Y, Mizutani K, et al. Protection against oxidative damage by dihydroflavonols in Engelhardtia chrysolepis. Biosci Biotechnol Biochem. 1996; 60:945–948. [PubMed: 8695910]
23. Kostyuk VA, Kraemer T, Sies H, Schewe T. Myeloperoxidase/nitrite-mediated lipid peroxidation of low-density lipoprotein as modulated by flavonoids. FEBS Lett. 2003; 537:146–150. [PubMed: 12606047]
24. Wang YH, Wang WY, Chang CC, Liou KT, Sung YJ, Liao JF, et al. Taxifolin ameliorates cerebral ischemia-reperfusion injury in rats through its anti-oxidative effect and modulation of NF-kappa B activation. J Biomed Sci. 2006; 13:127–141. [PubMed: 16283433]
25. Lee SB, Cha KH, Selenge D, Solongo A, Nho CW. The chemopreventive effect of taxifolin is exerted through ARE-dependent gene regulation. Biol Pharm Bull. 2007; 30:1074–1079. [PubMed: 17541156]
26. Brusselmans K, Vrolix R, Verhoeven G, Swinnen JV. Induction of cancer cell apoptosis by flavonoids is associated with their ability to inhibit fatty acid synthase activity. J Biol Chem. 2005; 280:5636–5645. [PubMed: 15533929]
27. Jung SK, Lee KW, Byun S, Kang NJ, Lim SH, Heo YS, et al. Myricetin suppresses UVB-induced skin cancer by targeting Fyn. Cancer Res. 2008; 68:6021–6029. [PubMed: 18632659]
28. Bode AM, Cho YY, Zheng D, Zhu F, Ericson ME, Ma WY, et al. Transient receptor potential type vanilloid 1 suppresses skin carcinogenesis. Cancer Res. 2009; 69:905–913. [PubMed: 19155296]
29. Schrödinger. Schrödinger Suite 2010. New York: Schrödinger, LLC; 2010.
30. Berman HM, Westbrook J, Feng Z, Gilliland G, Bhat TN, Weissig H, et al. The Protein Data Bank. Nucleic Acids Res. 2000; 28:235–242. [PubMed: 10592235]
31. Kwon JY, Lee KW, Kim JE, Jung SK, Kang NJ, Hwang MK, et al. Delphinidin suppresses ultraviolet B-induced cyclooxygenases-2 expression through inhibition of MAPKK4 and PI-3 kinase. Carcinogenesis. 2009; 30:1932–1940. [PubMed: 19776176]
32. Stamos J, Sliwkowski MX, Eigenbrot C. Structure of the epidermal growth factor receptor kinase domain alone and in complex with a 4-anilinoquinazoline inhibitor. J Biol Chem. 2002; 277:46265–46272. [PubMed: 12196540]
33. Berndt A, Miller S, Williams O, Le DD, Houseman BT, Pacold JI, et al. The p110 delta structure: mechanisms for selectivity and potency of new PI(3)K inhibitors. Nat Chem Biol. 2010; 6:117–124. [PubMed: 20081827]
34. Pettersen EF, Goddard TD, Huang CC, Couch GS, Greenblatt DM, Meng EC, et al. UCSF Chimera--a visualization system for exploratory research and analysis. J Comput Chem. 2004; 25:1605–1612. [PubMed: 15264254]
35. Wakeling AE, Guy SP, Woodburn JR, Ashton SE, Curry BJ, Barker AJ, et al. ZD1839 (Iressa): an orally active inhibitor of epidermal growth factor signaling with potential for cancer therapy. Cancer Res. 2002; 62:5749–5754. [PubMed: 12384534]
36. Ashida M, Bito T, Budiyanto A, Ichihashi M, Ueda M. Involvement of EGF receptor activation in the induction of cyclooxygenase-2 in HaCaT keratinocytes after UVB. Exp Dermatol. 2003; 12:445–452. [PubMed: 12930301]
37. Chen W, Tang Q, Gonzales MS, Bowden GT. Role of p38 MAP kinases and ERK in mediating ultraviolet-B induced cyclooxygenase-2 gene expression in human keratinocytes. Oncogene. 2001; 20:3921–3926. [PubMed: 11439356]
38. Ibuki Y, Goto R. Suppression of apoptosis by UVB irradiation: survival signaling via PI3-kinase/Akt pathway. Biochem Biophys Res Commun. 2000; 279:872–878. [PubMed: 11162442]
39. Vega-Villa KR, Remsberg CM, Ohgami Y, Yanez JA, Takemoto JK, Andrews PK, et al. Stereospecific high-performance liquid chromatography of taxifolin, applications in pharmacokinetics, and determination in tu fu ling (Rhizoma smilacis glabrae) and apple (Malus x domestica). Biomed Chromatogr. 2009; 23:638–646. [PubMed: 19267323]

40. Japon-Lujan R, Luque de Castro MD. Static-dynamic superheated liquid extraction of hydroxytyrosol and other biophenols from alperujo (a semisolid residue of the olive oil industry). J Agric Food Chem. 2007; 55:3629–3634. [PubMed: 17411068]

41. Kiehlmann E, Slade PW. Methylation of dihydroquercetin acetates: synthesis of 5-O-methyldihydroquercetin. J Nat Prod. 2003; 66:1562–1566. [PubMed: 14695797]

42. Chen L, Yin Y, Yi H, Xu Q, Chen T. Simultaneous quantification of five major bioactive flavonoids in Rhizoma smilacis glabrae by high-performance liquid chromatography. J Pharm Biomed Anal. 2007; 43:1715–1720. [PubMed: 17291706]

43. Dubois RN, Abramson SB, Crofford L, Gupta RA, Simon LS, Van De Putte LB, et al. Cyclooxygenase in biology and disease. Faseb J. 1998; 12:1063–1073. [PubMed: 9737710]

44. Pentland AP, Schoggins JW, Scott GA, Khan KN, Han R. Reduction of UV-induced skin tumors in hairless mice by selective COX-2 inhibition. Carcinogenesis. 1999; 20:1939–1944. [PubMed: 10506108]

45. Kuper C, Beck FX, Neuhofer W. Toll-like receptor 4 activates NF-kappaB and MAP kinase pathways to regulate expression of proinflammatory COX-2 in renal medullary collecting duct cells. Am J Physiol Renal Physiol. 2012; 302:F38–F46. [PubMed: 21937604]

46. Sheu ML, Chao KF, Sung YJ, Lin WW, Lin-Shiau SY, Liu SH. Activation of phosphoinositide 3-kinase in response to inflammation and nitric oxide leads to the up-regulation of cyclooxygenase-2 expression and subsequent cell proliferation in mesangial cells. Cell Signal. 2005; 17:975–884. [PubMed: 15894170]

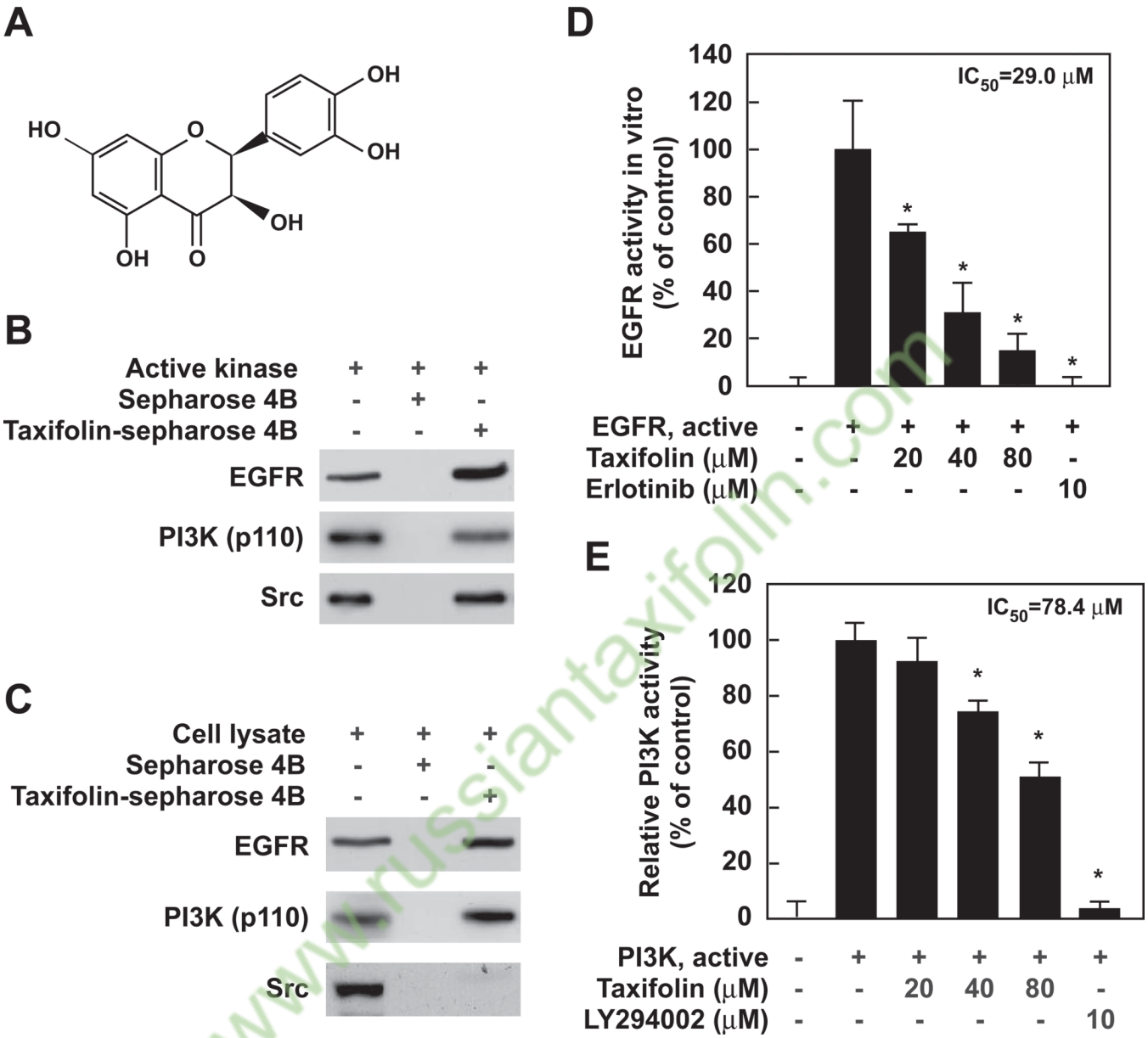

Figure 1.

EGFR and PI3-K are important targets of taxifolin. *A*, chemical structure of taxifolin. *B*, taxifolin binds to EGFR, PI3-K and Src *in vitro*. Active EGFR, PI3-K or Src (200 ng) was incubated with taxifolin-conjugated Sepharose 4B beads or Sepharose 4B beads alone, and the pulled-down proteins were analyzed by Western blot. *C*, taxifolin binds to EGFR and PI3-K but not to Src *ex vivo*. Cell lysates from JB6 P+ cells (500 μg) were incubated with taxifolin-conjugated Sepharose 4B beads or Sepharose 4B beads, and the pulled-down proteins were analyzed by Western blot. *B* and *C*, data are representative of three independent experiments that gave similar results. *D*, taxifolin inhibits EGFR kinase activity *in vitro*. Active EGFR (100 ng) was mixed with taxifolin (0, 20, 40 or 80 μM) or erlotinib (EGFR inhibitor, 10 μM) and then incubated with a [γ-^{32}P] ATP mixture. The radioactive incorporation was determined using a scintillation counter. *E*, taxifolin inhibits PI3-K kinase activity *in vitro*. Active PI3-K (100 ng) was mixed with taxifolin (0, 20, 40 or 80 μM) or LY294002 (PI3-K inhibitor, 10 μM) and then incubated with a [γ-^{32}P] ATP mixture.

The ^{32}P-labeled PI3P was separated by TLC and then visualized by autoradiography. *D* and *E*, data are represented as means ± S.D. from three independent experiments performed with triplicate samples and significance was determined by the Student's *t*-test. The asterisk (*) indicates a significant decrease versus EGFR or PI3-K alone ($P < 0.05$).

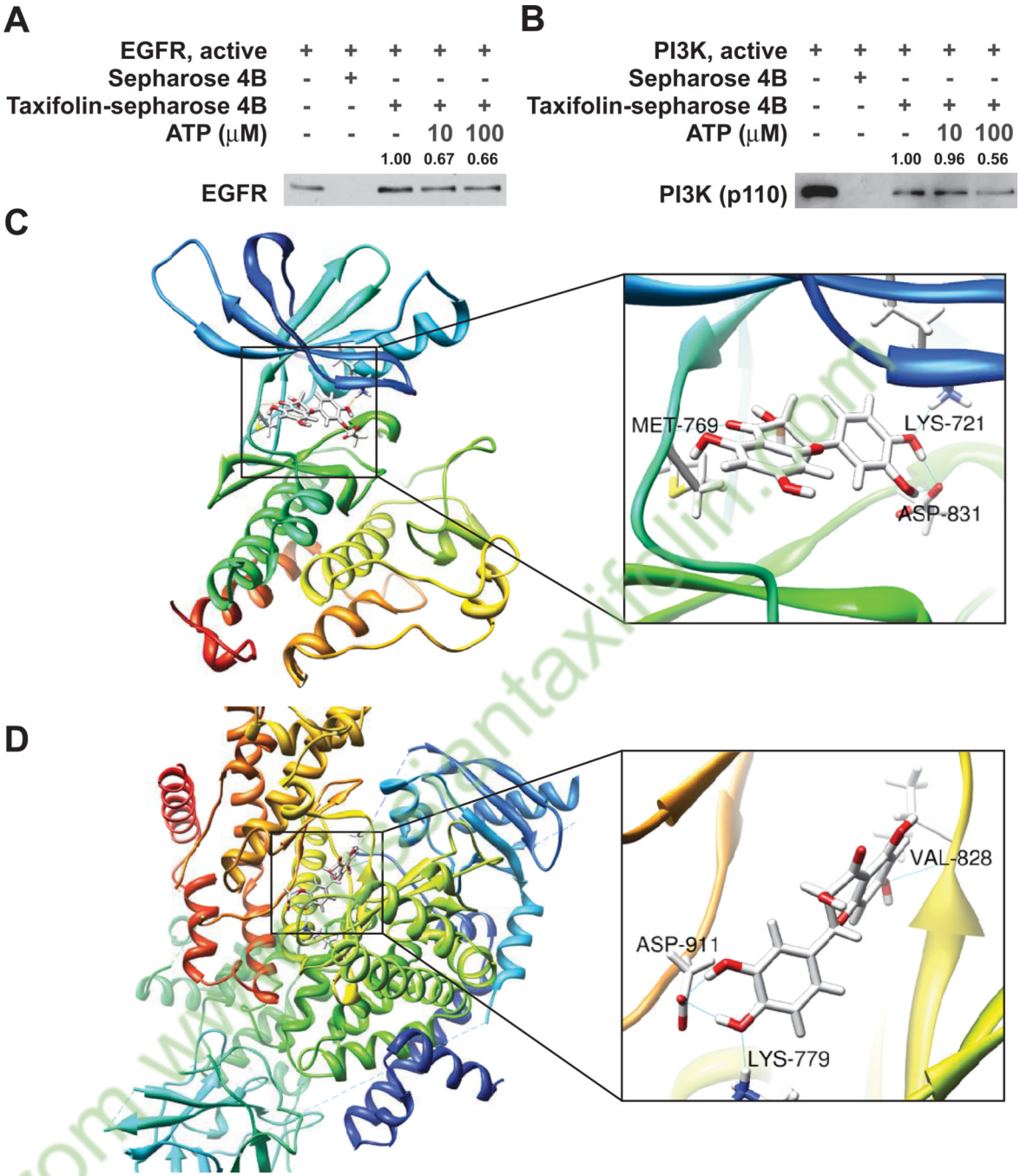

Figure 2.

Taxifolin binds to EGFR and PI3-K at the ATP-binding pocket. *A*, taxifolin binds with EGFR in an ATP-competitive manner. *B*, taxifolin binds with PI3-K in an ATP-competitive manner. Active EGFR or PI3-K (200 ng) was incubated with different concentrations of ATP (0, 10 or 100 μM) and then incubated with taxifolin-conjugated Sepharose 4B beads or Sepharose 4B beads. The pulled-down proteins were analyzed by Western blot. Data are representative of three independent experiments that gave similar results. *C*, docking model of EGFR and taxifolin. *D*, docking model of PI3-K and taxifolin. Docking models show the predicted interactions.

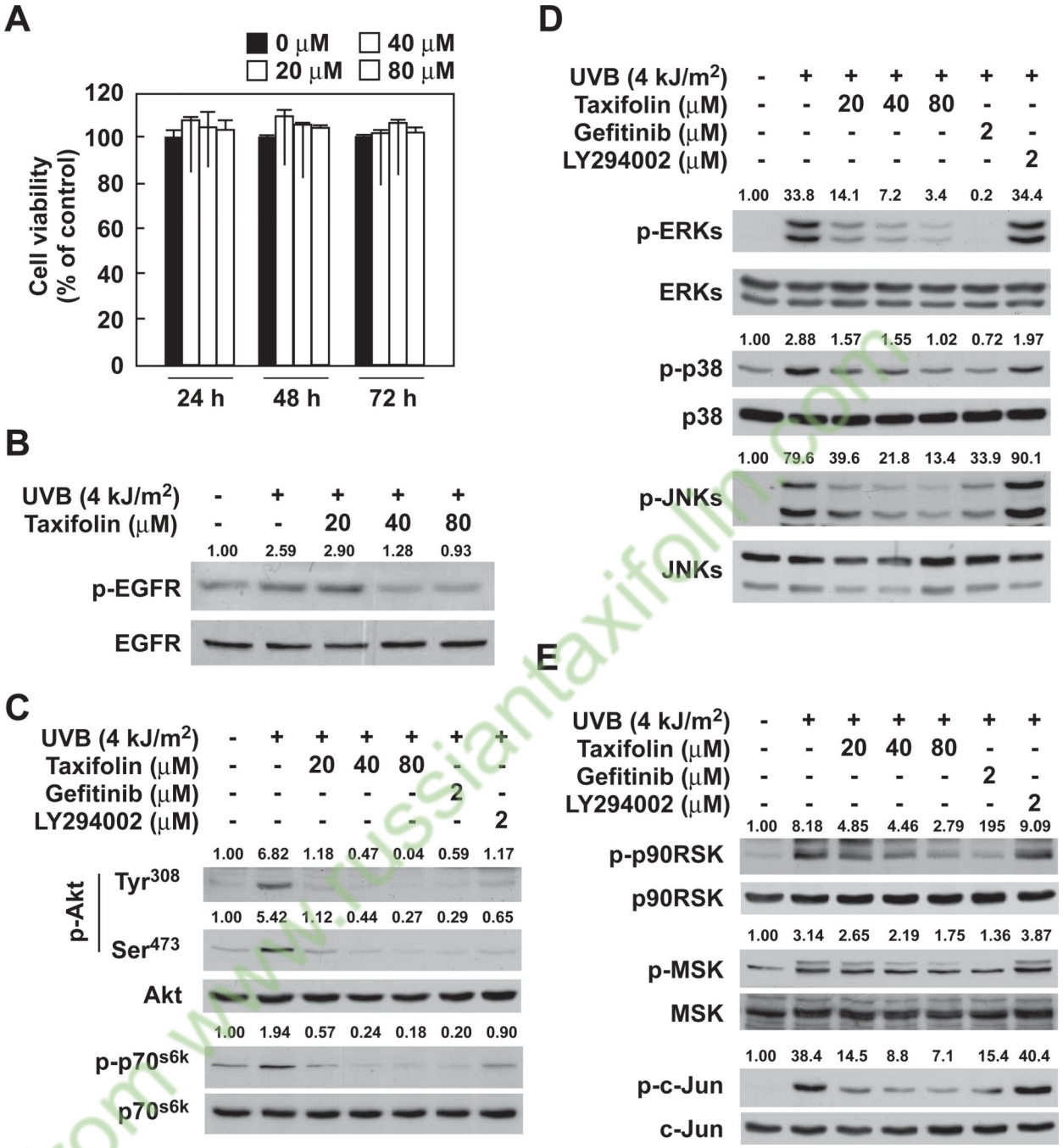

Figure 3.

Taxifolin suppresses UVB-induced phosphorylation of the EGFR and PI3-K/Akt signaling pathways. *A*, taxifolin has no toxicity on JB6 P+ cells. JB6 P+ cells were treated with taxifolin (0, 20, 40 or 80 μM) for 24, 48 or 72 h. Data are represented as means ± S.D. from three independent experiments performed with triplicate samples and significance was determined by the Student's *t*-test. No significant difference was observed between any groups. *B*, taxifolin inhibits UVB-induced phosphorylation of EGFR. *C*, taxifolin inhibits UVB-induced phosphorylation of PI3-K/Alt signaling proteins. *D*, taxifolin inhibits UVB-induced phosphorylation of ERKs, p38 and JNKs. *E*, taxifolin inhibits UVB-induced phosphorylation of p90RSK, MSK and c-Jun. *B-E*, JB6 P+ cells were starved in serum-free

MEM and treated with taxifolin (0, 20, 40 or 80 μM), gefitinib (2 μM) or LY294002 (2 μM) for 24 h before being exposed to UVB (4 kJ/m^2). After incubation for 5 min (B), 15 min (C and D) or 30 min (E), cells were harvested and the levels of phosphorylated and total proteins were determined by Western blot. Data are representative of three independent experiments that gave similar results.

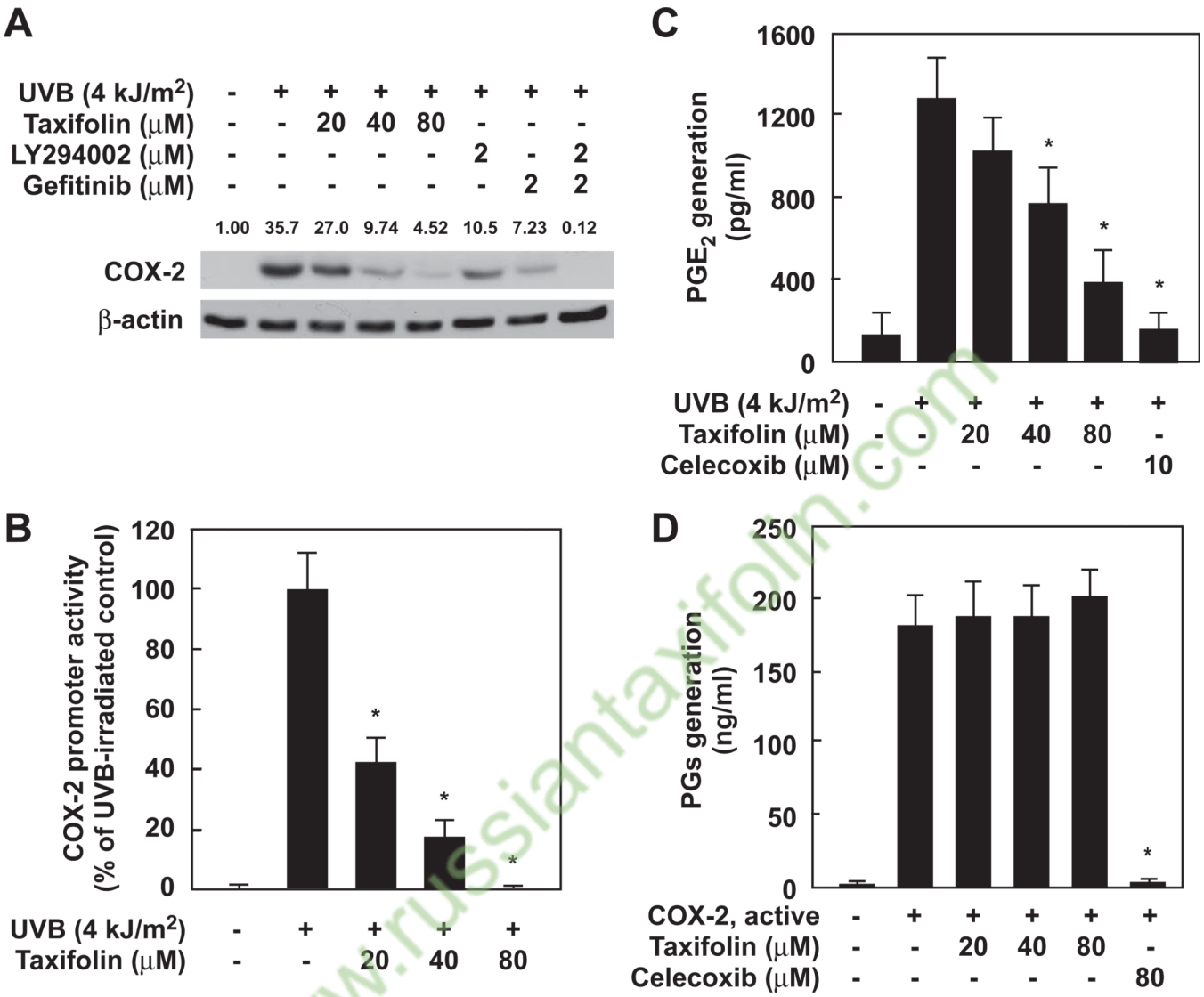

Figure 4.

Taxifolin suppresses UVB-induced expression and promoter activity of *COX-2*, and PGE_2 generation. *A*, taxifolin, as well as inhibitors of EGFR or PI3-K, suppress UVB-induced COX-2 expression. Cells were starved in serum-free MEM and then treated with taxifolin (0, 20, 40 or 80 μM), gefitinib (2 μM) and/or LY294002 (2 μM) for 24 h before being exposed to UVB (4 kJ/m^2). After incubation for 4 h, the cells were harvested and the levels of COX-2 and β-actin were determined. Data are representative of three independent experiments that gave similar results. *B*, taxifolin suppresses the promoter activity of *COX-2* induced by UVB. JB6 P+ cells stably transfected with a *COX-2 luciferase reporter* plasmid were starved in serum-free medium and then treated with taxifolin (0, 20, 40 or 80 μM) for 1 h before exposure to UVB (4 kJ/m^2). After incubation for 12 h, luciferase activity was measured. *C*, taxifolin suppresses PGE_2 generation induced by UVB. Cells were starved in serum-free MEM and then treated with taxifolin (0, 20, 40 or 80 μM) or celecoxib (COX-2 inhibitor, 10 μM) for 1 h before being exposed to UVB (4 kJ/m^2). After incubation for 6 h, PGE_2 generation in the medium was determined using a PGE_2 EIA kit. *D*, taxifolin has no effect on COX-2 activity *in vitro*. *In vitro* COX-2 activity was determined using the COX Inhibitor Screening Assay kit. *B–D*, data are represented as means ± S.D. from three

independent experiments performed with triplicate samples and significance was determined by the Student's *t*-test. The asterisk (*) indicates a significant decrease versus UVB (*B and C*) or COX-2 (*D*) alone ($P < 0.05$).

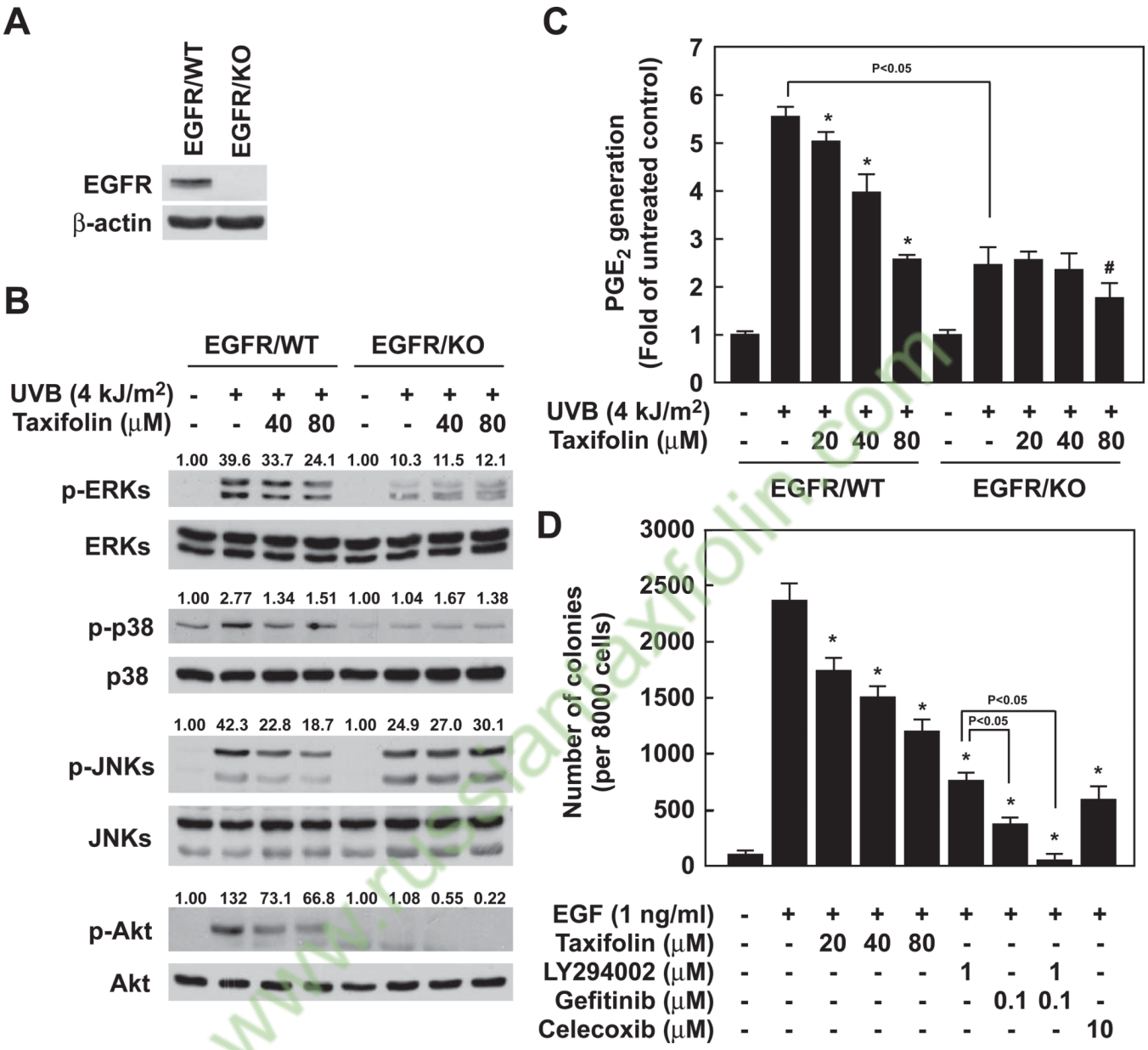

Figure 5.

The effect of taxifolin was reduced in EGFR/KO MEFs compared with EGFR/WT MEFs. *A*, EGFR expression is only detectable in EGFR/WT MEFs. *B*, the effect of taxifolin on UVB-induced phosphorylation of signaling proteins is reduced in EGFR/KO MEFs compared with EGFR/WT MEFs. EGFR/WT or KO MEFs were starved in serum-free DMEM and then treated with taxifolin (0, 40 or 80 μM) for 24 h before being exposed to UVB (4 kJ/m^2). After incubation for 15 min, the cells were harvested and the levels of phosphorylated and total proteins were determined by Western blot. *A* and *B*, data are representative of 3 independent experiments that gave similar results. *C*, the effect of taxifolin on PGE_2 generation is reduced in EGFR/KO MEFs compared with EGFR/WT MEFs. EGFR/WT or KO MEFs were starved in serum-free DMEM and then treated with taxifolin (0, 20, 40 or 80 μM) for 1 h before being exposed to UVB (4 kJ/m^2). After incubation for 6 h, PGE_2 generation in the medium was determined using a PGE_2 EIA kit.

Data are represented as means ± S.D. from three independent experiments performed with triplicate samples and significance was determined by the Student's *t*-test. The asterisk (*) or (#) indicates a significant decrease versus UVB alone in EGFR/WT or KO MEFs, respectively ($P < 0.05$). *D*, taxifolin, as well as inhibitors, of EGFR, PI3-K or COX-2 suppresses EGF-induced cell transformation. JB6 P+ cells were treated with taxifolin (0, 20, 40 or 80 μM), gefitinib (0.1 μM), LY294002 (1 μM) or celecoxib (10 μM) together with 1 ng/ml EGF on solidified BME supplemented with 10% FBS and 0.5% agar. After incubation for 7 days, colonies were counted. Data are represented as means ± S.D. from three independent experiments performed with triplicate samples and significance was determined by the Student's *t*-test. The asterisk (*) indicates a significant decrease versus EGF alone ($P < 0.05$).

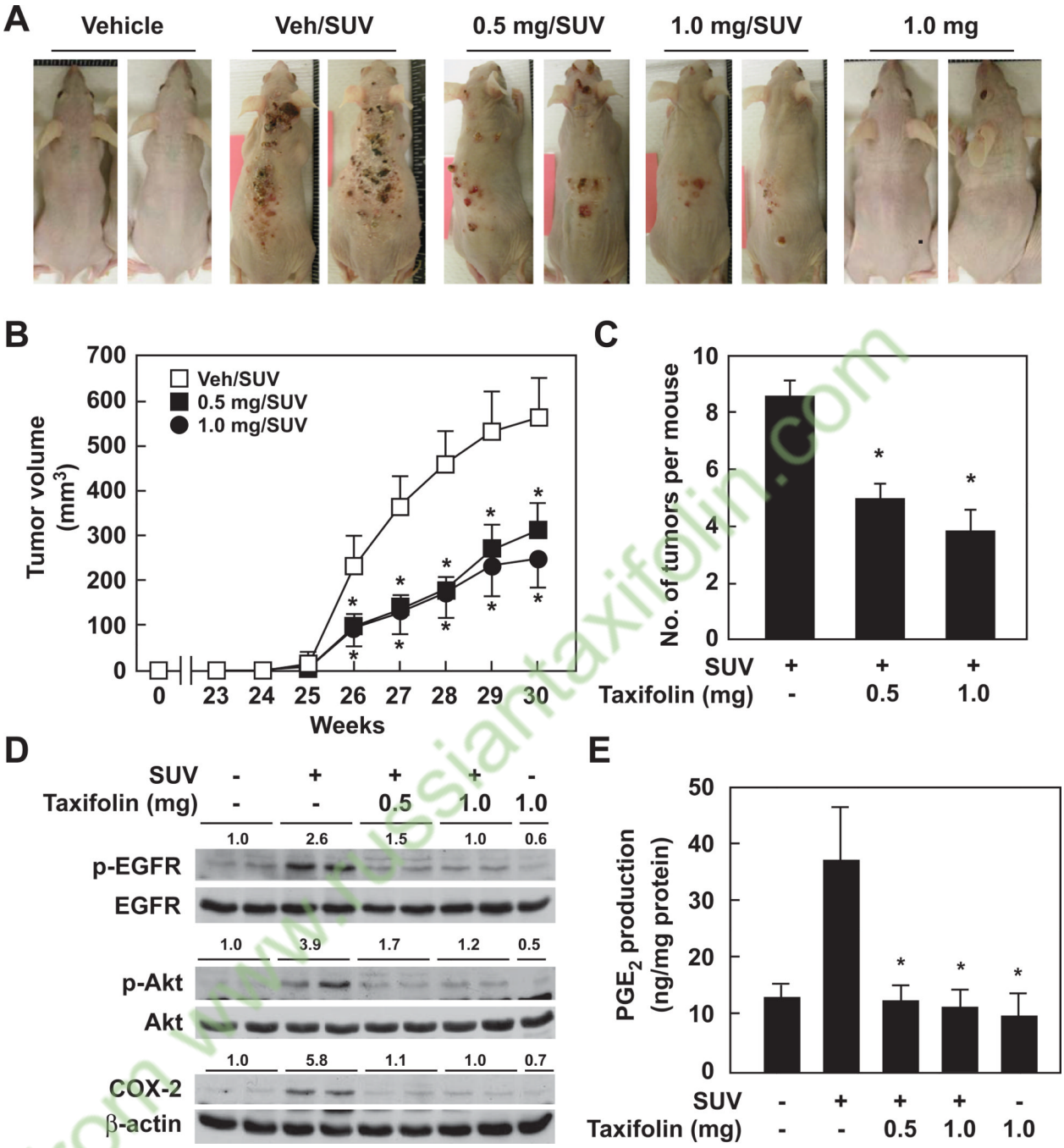

Figure 5.

Taxifolin suppresses SUV-induced skin carcinogenesis *in vivo*. SKH-1 hairless mice were treated as described in Materials and Methods. The mice in the vehicle group (n = 10) received topical treatment with acetone only. The mice in the 1.0 mg taxifolin group (n = 10) were treated with 1.0 mg taxifolin only. In the Veh/SUV group (n = 20), the mice were treated with acetone before SUV exposure. The mice in the 0.5 mg/SUV or 1.0 mg/SUV groups (n = 20 each) received treatment with taxifolin (0.5 or 1.0 mg, respectively) before SUV exposure. The frequency of irradiation was set at 3 times a week for 15 weeks. The respective doses of acetone or taxifolin were applied topically to the dorsal area. Tumor incidence and multiplicity were recorded weekly until the end of the experiment at week 30.

A, external appearance of tumors. *B*, taxifolin suppresses SUV-induced tumor volume. Tumor volume was calculated according to the following formula: tumor volume (mm^3) = length × width × height × 0.52. *C*, taxifolin suppresses SUV-induced tumor number per mouse at the end of experiment (week 30). *B* and *C*, data are represented as means ± S.E. and differences were determined by one-way ANOVA. The asterisk (*) indicates a significant decrease versus the Veh/SUV group ($P < 0.01$). *D*, taxifolin inhibits SUV-induced phosphorylation of EGFR and Akt, and COX-2 expression in mouse skin. The expression levels of phosphorylated and total proteins were analyzed by Western blot. *E*, taxifolin suppresses SUV-induced PGE_2 production in mouse skin. PGE_2 production was determined using a PGE_2 EIA kit and the amount of PGE_2 is expressed as ng/mg protein. *D* and *E*, data are represented as means ± S.D. and significance was determined by the Student's *t*-test. The asterisk (*) indicates a significant decrease versus SUV alone ($P < 0.05$).